ER bodies are induced by *Pseudomonas syringae* and negatively regulate immunity

Running title: Role of ER bodies in the defense response

José S. Rufián[1,2,3], James M. Elmore[2,4], Eduardo R. Bejarano[1], Carmen R. Beuzon[1], Gitta L. Coaker[2*]

[1] Instituto de Hortofruticultura Subtropical y Mediterránea, Universidad de Málaga-Consejo Superior de Investigaciones Científicas (IHSM-UMA-CSIC), Depto. Biología Celular, Genética y Fisiología, Campus de Teatinos, Málaga E-29071, Spain

[2] Department of Plant Pathology, University of California Davis, Davis, CA 95616 USA

[3] Current address: Shanghai Center for Plant Stress Biology, Shanghai Institutes of Biological Sciences, Chinese Academy of Sciences, Shanghai 201602, China

[4] Current address: Department of Plant Pathology and Microbiology, Iowa State University, Ames, IA 5001 USA

*Address correspondence to: glcoaker@ucdavis.edu

ABSTRACT

ER bodies are endoplasmic reticulum-derived organelles present in plants belonging to the *Brassicales* order. In *Arabidopsis thaliana*, ER bodies are ubiquitous in cotyledons and roots, and present only in certain cell types in rosette leaves. However, both wounding and jasmonic acid treatment induce the formation of ER bodies in leaves. Formation of this structure is dependent on the transcription factor *NAI1*. The main components of the ER bodies are β-glucosidases (BGLUs), enzymes that hydrolyze secondary compounds. In *Arabidopsis*, PYK10 (BGLU23) and BGLU18 are the most abundant ER body proteins. In this work, we found that ER bodies are downregulated as a consequence of the immune responses induced by bacterial flagellin perception. *Arabidopsis* mutants defective in ER body formation show enhanced responses upon flagellin perception and enhanced resistance to bacterial infections. Furthermore, the bacterial toxin coronatine induces the formation of *de novo* ER bodies in leaves and its virulence function is partially dependent on this structure. Finally, we show that performance of the polyphagous beet armyworm herbivore, *Spodoptera exigua*, increases in plants lacking ER bodies. Altogether, we provide new evidence for the role of the ER bodies in plant immune responses.

Keywords: ER bodies, plant immunity, *Pseudomonas syringae*, *Spodoptera exigua*,

INTRODUCTION

ER bodies are rod-shaped endoplasmic reticulum (ER)-associated structures that are present in three families within the Brassicales order (Nakano et al. 2014a). ER bodies are constitutively present in roots and cotyledons of young plants (constitutive ER bodies), but their abundance decreases with senescence (Matsushima et al. 2002). In *Arabidopsis* rosette leaves, ER bodies are constitutively present in marginal cells, epidermal cells covering the midrib and extremely large pavement cells (Leaf ER bodies) (Nakazaki et al. 2019b). Furthermore, the formation of ER bodies in rosette leaves is induced by Methyl Jasmonate (MeJa) treatment or wounding (Inducible ER bodies) (Matsushima et al. 2002).

Formation of ER bodies is dependent on the basic-helix-loop-helix transcription factor *NAI1* (Matsushima et al. 2004) and the essential protein *NAI2* (Yamada et al. 2008). The main components of the constitutive ER bodies are the β-glucosidases (BGLU) PYK10 (BGLU23), BGLU21 and BGLU22 (Matsushima et al. 2003), while induced-ER bodies also contain BGLU18 (Ogasawara et al. 2009). These myrosinases belong to a subfamily of 8 β-glucosidases (*i. e.* BGLU18 to BGLU25) (Xu et al. 2004) with ER-retention signals (Yamada et al. 2011). Leaf ER bodies mainly contain PYK10 and BGLU18 (Nakazaki et al. 2019b). PYK10 has been described as an atypical myrosinase that hydrolyzes Indole Glucosinolates (IG) (Nakano et al. 2017). Upon tissue disruption, PYK10 associates in the cytosol with PYK10-binding protein 1 (PBP1), activating PYK10 function (Nagano et al. 2005). An *Arabidopsis pyk10/blgu18* double mutant accumulates high amounts of the IG 4-methoxyindol-3-ylmethylglucosinolate (4MI3G) after tissue disruption (Nakazaki et al. 2019b). IGs and the products resulting from their breakdown

have a role in the defense responses against microbial pathogens and herbivory (Bednarek et al. 2009; Clay et al. 2009; Johansson et al. 2014; Millet et al. 2010; Müller et al. 2010; Nakazaki et al. 2019b). IGs are also required for the establishment of beneficial interactions with the endophytic fungus *Pirimospora indica* by appropriately regulating the level of root colonization through *PYK10* (Lahrmann et al. 2015; Sherameti et al. 2008). Collectively, multiple independent studies have supported a role in defense responses for ER bodies (Nakano et al. 2014b; Yamada et al. 2011).

Plants are constantly exposed to a variety of biotic and abiotic stresses. Surface localized plant pattern-recognition receptors (PRRs) act as one of the first lines of defense against pathogens and are able to recognize conserved pathogen features, such as flagellin, as non-self (Couto and Zipfel 2016). One of the best-characterized PRRs is the flagellin receptor FLS2 (Flagellin Sensing 2) which recognizes flg22, a 22 amino acid epitope of bacterial flagellin (Gómez-Gómez and Boller 2000). Perception of flg22 by FLS2 induces a number of cellular events resulting in Pattern-Triggered Immunity (PTI), which restricts pathogen proliferation. Some of the cellular events that take place during PTI are the activation of MAP Kinases (MAPK) and calcium-dependent protein kinases, the production of reactive oxygen species (ROS), stomatal closure and the formation of callose (β-1,3-glucan) deposits in the cell wall (Henry et al. 2013). However, successful pathogens have evolved different mechanisms to suppress defense responses and successfully colonize their host.

Pseudomonas syringae is a Gram-negative bacterium that has been extensively used to study plant immune signaling. *P. syringae* virulence depends on the Type Three Secretion System (T3SS), a complex nanomachine that translocates proteins, called

effectors, into the cytosol of the plant cell. Most of the effectors suppress PTI acting on different cellular pathways (Macho 2015). Another virulence mechanisms used by bacterial pathogens to subvert plant immunity is the production of phytotoxins. *P. syringae* pv. tomato DC3000 produces coronatine, a polyketide toxin that acts as a molecular mimic of the plant hormone jasmonic acid (JA) (Weiler et al. 1994). Coronatine induces stomata re-opening upon PRR perception to allow bacterial colonization (Gimenez-Ibanez et al. 2017; Melotto et al. 2008; Melotto et al. 2006), and also suppresses callose deposition and induces bacterial growth within the apoplast (Geng et al. 2012).

In this work, we investigated the biological function of ER bodies during plant immunity. We found that ER bodies are downregulated after flg22-triggered immune activation but induced after *P. syringae* infection in a coronatine-dependent manner. Furthermore, loci underlying ER body formation act as negative regulators of immunity against bacterial pathogens but are required for a complete response against the chewing insect *Spodoptera exigua.* With these results, we report a new and contrasting role of ER bodies in defense against phytopathogenic bacteria and chewing insects.

RESULTS

ER bodies are rapidly inhibited upon flagellin perception

To investigate the role of ER body formation after plant immune perception, we used an *Arabidopsis* transgenic line expressing GFP with the ER-retention signal HDEL (GFP-HDEL), which allows the visualization of ER bodies (Mitsuhashi et al. 2000). We vacuum-infiltrated 2 week-old *Arabidopsis* plants with either 10 µM flg22 or water and visualized cotyledons three hours later by confocal microscopy. We were able to detect and quantify the ER bodies in cotyledons, where this structure is constitutively present, in mock-treated plants. However, after flg22 treatment, only a small number of ER bodies were detected (Fig. 1A). This decrease in ER body detection was statistically different compared to water-treated controls (Fig. 1A). Treatment with flg22 had no effect in the *nai1-1* GFP-HDEL mutant, which lacks ER bodies in cotyledons (Fig S1).

To analyze the impact of the flg22 treatment in ER body formation at the transcriptional level, we analyzed the transcriptional expression of *NAI1* and *PYK10* under different biotic treatments using an available dataset (NASCArrays-120). We found that flg22 treatment reduces the expression level of *NAI1*, pointing to regulation of ER bodies at the transcriptional level as a consequence of activation of defense responses. However, inoculation with the virulent bacterial strain *P. syringae* DC3000 induces the expression of both *NAI1* and *PYK10* at 24h, and the same occurs with a strain expressing the avirulence effector AvrRpm1 (Fig 1B). Interestingly, both the T3SS mutant derivative Δ*hrcC* and the non-host strain 1448A reduced the accumulation of *NAI1* transcripts (Fig 1B). Altogether, these results show a downregulation of ER bodies as a consequence of

the activation of flg22-triggered immunity and suggest a role of this subcellular structure during the defense response against *P. syringae*.

Arabidopsis mutants impacting ER body formation and contents exhibit enhanced immune responses against bacterial pathogens

After flg22 perception, many cellular events take place to restrict pathogen invasion, including activation of MAPKs and calcium dependent protein kinases minutes after perception, followed by ROS production, activation of defense gene expression and several hours later, callose deposition (Henry et al. 2013). To further characterize the role of the ER bodies in flg22-induced responses, we measured ROS production as an early event of PTI, in plants affected in the formation of ER bodies. We treated 3-week-old Col-0, *nai1-1, pyk10-1* and *pyk10-1/blgu21* plants, with 100 nM flg22 and measured the ROS burst. The total ROS produced in all the mutant backgrounds tested was higher than the ROS produced in Col-0 (Fig. 2A). This increase in ROS production in response to flg22 also occurs in both *bglu18-1* and *pbp1-1* mutants (Fig S2A). To analyze a late event of PTI, we treated four-week-old plants with flg22 and quantified callose deposition. Consistent with the ROS burst, the number of callose deposit was two times higher in ER bodies mutants compared to Col-0 (Fig 2B). These data indicate that a loss of ER bodies or its main components induce an enhanced response to bacterial flg22, pointing to a negative role of ER bodies on PTI.

To determine the role of the ER bodies in bacterial growth, we quantified DC3000 titers in Col-0 and in the different mutant backgrounds (Fig. 2C). DC3000 exhibited decreased growth (>1 log) in the *nai1-1* mutant compared to Col-0. Interestingly, both the *pyk10-1*

and the *pyk10-1/bglu21* mutants exhibited a stronger decrease in bacterial growth, with 1.5 Log reduction compared to wild-type Col-0 (Fig 2C). No differences were detected between *pyk10* and *pyk10-1/bglu21*, indicating that *PYK10* is a critical gene involved in negative regulation of bacterial growth. Plants lacking *pbp1*, necessary for PYK10 function, or *bglu18*, the main component of inducible ER bodies, also showed enhanced resistance to bacterial infection (Fig S2B).

A critical component controlling bacterial virulence is the ability to deliver effectors through the type III secretion system (Macho 2015). In order to investigate the relationship between immune suppression and ER body formation, we used DC3000 Δ*hrcC*, which is unable to translocate effectors to the plant cell, and thus, does not suppress PTI. We measured the growth of Δ*hrcC* in ER body mutants. In the *nai1-1* background, the growth of Δ*hrcC* was not significantly different from that in Col-0. However, we observed a slight but significant decrease in growth in the *pyk10-1/bglu21* background (Fig 2D). The increased *P. syringae* growth restriction in *pyk10-1* and *pyk10-1/bglu21* backgrounds compared with *nai1* (Fig 2C and 2D) could indicate a NAI1-independent regulation for *PYK10* and/or *BGLU21*. Altogether, these results show that the absence of ER bodies increases resistance against the bacterial pathogen *P. syringae.*

Coronatine induces the formation of ER bodies in rosette leaves

Transcriptomic analyses indicate that inoculation with virulent DC3000 induces the expression of *nai1* and *pyk10* (Fig 1B). To check if this increased expression results in *de novo* formation of ER bodies, we inoculated rosette leaves of *Arabidopsis* GFP-HDEL plants with a concentrated suspension ($5x10^7$ CFU/mL) of DC3000, the derivative Δ*hrcC*

and a coronatine mutant (*cor*-). Three days after inoculation, we observed the samples under the confocal microscope (Fig 3A). No ER bodies were found in the mock-treated leaves, in agreement to the described absence of ER bodies in certain rosette leaves (Matsushima et al. 2002; Nakazaki et al. 2019b). Interestingly, a large number of ER bodies was found in leaves inoculated with wild-type DC3000. The distribution of the ER bodies was patchy, suggesting that only some cells were forming the structure. To investigate if the formation of ER bodies localized surrounding bacterial colonies, we generated a DC3000 derivative tagged with eYFP. Three days after inoculation, we observed a vast number of ER bodies surrounding the bacterial microcolony (Fig 3B). To determine which bacterial factors are inducing the formation of ER bodies in rosette leaves, we inoculated the Δ*hrcC* derivative and the *cor*- mutant, both tagged with eYFP. We were unable to detect Δ*hrcC* –eYFP microcolonies due to their extremely small size, consistent with their reduced growth *in planta*. Nevertheless, we did not detect ER bodies in leaves inoculated with the Δ*hrcC* mutant (Fig. 3A). Interestingly, the *cor*- eYFP mutant was unable to induce the formation of *de novo* ER bodies, consistent with the role of coronatine mimicking JA (Fig. 3). This result indicates that induction of ER bodies could be a virulence function of coronatine. Analyzing transcriptomic data of plants inoculated either with DC3000 or the *cor*- mutant, we observed that many genes related to ER bodies, including *NAI1*, *PYK10* and *BGLU18*, were upregulated by DC3000 but not after inoculation with DC3000 *cor*- (Fig. S3). To investigate the ability of coronatine to promote bacterial virulence in the absence of ER body formation, we measured the growth of DC3000 and the DC3000 *cor*- mutant in Col-0, *nai1-1*, *pyk10-1* and *pyk10-1/bglu21*. In order to bypass the role of coronatine on re-opening stomata (Melotto et al. 2008; Melotto

et al. 2006), we performed syringe inoculation in five-week old plant leaves. Four days after inoculation, a strong growth restriction was observed in the coronatine mutant compared with wild-type DC3000 in Col-0 (Fig 3C). In the ER body-defective backgrounds, a stronger growth restriction was observed for DC3000 (Fig 2C, Fig 3C). However, the growth of the coronatine mutant was not significantly different between wild-type Col-0 and the ER body mutants.

NAI1* contributes to the defense response against *S. exigua

ER bodies have been proposed to participate in the defense response against herbivores (Nakano et al. 2014b; Yamada et al. 2011). A recent study demonstrated increased susceptibility of the double mutant *bglu18 pyk10* to the terrestrial isopod *Armadillidium vulgare* (Nakazaki et al. 2019b). We measured the performance of the generalist leaf-chewing herbivore *S. exigua* in different ER body related mutants. Performance assays have been widely used to study the defense mechanisms against herbivory (Chung et al. 2008; Cipollini et al. 2004; Müller et al. 2010; Santamaría et al. 2017; Van Oosten et al. 2008). We fed *Spodoptera exigua* larvae with Col-0 and the ER body-defective mutants *nai1-1*, *pyk10-1* and *pyk10-1/bglu21* plants, and measured the weight of the larvae after 7 days. The fresh weight of *S. exigua* larvae was higher in *nai1-1* plants compared with the Col-0 control, confirming a role of ER bodies in the defense response against herbivore insects. Surprisingly, the performance of *S. exigua* in either *pyk10-1* or *pyk10-1/bglu21* plants was not different compared Col-0, suggesting a redundant role of PYK10 and BGLU21 with other myrosinases in this context.

DISCUSSION

The main contents in ER bodies are β -glucosidases, enzymes which can produce toxic compounds to protect the plant from herbivore attack (Matsushima et al. 2003). Induction of ER bodies by wounding or by MeJa treatment suggests an association with plant defense (Nakano et al. 2014b). However, there are few experimental evidences of the association between ER bodies and plant immunity. Plants are infected by diverse pathogens that often utilize opposing virulence strategies and are differentially impacted by plant immune responses (e.g. chewing insects versus biotrophic pathogens). In this study we demonstrate contrasting roles of ER bodies in the plant response to pathogenic bacteria and herbivores.

Previous studies have implicated ER bodies in plant protection against fungi and feeding insects. Sherameti et al. (2008) demonstrated that *PYK10* is required to protect plants against excessive root colonization by the endophytic fungus *Pirimormospora indica.* Furthermore, Nakazaki et al. (2019b) showed that *bglu18 pyk10* double mutant plants are more susceptible than wild-type to the attack of the terrestrial isopod *Armadillidium vulgare* (pill-bug). In this work, we experimentally link the function of the ER bodies with the plant response against the bacterial pathogen *P. syringae* and the herbivore *S. exigua*. We found an increased weight acquisition of the generalist chewing herbivore *S. exigua* in *nai1-1* plants compared with Col-0, but not in *pyk10-1* and *pyk10-1/bglu21* mutants (Fig. 4). *S. exigua* feeds on leaves, where constitutive ER bodies are absent (Matsushima et al. 2002). Leaf ER bodies, which are dependent on *NAI1*, localize in the edges of the leaves and mainly contain PYK10 and BGLU18 (Nakazaki et al. 2019b). The biogenesis and content of leaf ER bodies is regulated by both Jasmonic Acid (JA)

dependent and independent pathways (Nakazaki et al. 2019a). While *NAI1* expression, and therefore PYK10 accumulation is dependent on JA, BGLU18 accumulation in leaf ER bodies is independent on JA (Nakazaki et al. 2019a). Since the performance of *S. exigua* is not affected in *pyk10-1* mutant, the genetic analysis points to *BGLU18* as the responsible of the defense response against *S. exigua*. Furthermore, chewing induces JA accumulation (Rehrig et al. 2014) and this signal would potentially lead to the formation of the inducible ER bodies, which are independent of NAI1 and mainly contain BGLU18.

P. syringae pv. *tomato* induces the formation of ER bodies in leaves. Since the flagellin peptide flg22 downregulates the formation of constitutive ER bodies and we have shown that ER bodies negatively regulate PTI, we hypothesize that *P. syringae*-induction of ER bodies is a virulence strategy to suppress host immune responses. The two main virulence factors of *P. syringae* pv. tomato are the phytotoxin coronatine and the T3SS. The bacterial phytotoxin coronatine, which mimics the function of JA in the plant (Bender et al. 1999), induces the formation of ER bodies in leaves (Fig 3A,B). The main virulence function of coronatine is to re-open stomata upon PAMP-induced closure (Melotto et al. 2008; Melotto et al. 2006). However, coronatine also has been shown to suppress immunity once the bacteria colonize the apoplast (Fig 3C; (Geng et al. 2012)). The T3SS defective mutant Δ*hrcC* is not able to induce the formation of ER bodies, which would indicate an effect of T3Es on the induction of ER bodies. However, we cannot rule out that the absence of ER bodies is due to an insufficient amount of coronatine produced by the Δ*hrcC* microcolonies.

Bacterial flg22 perception leads to a down regulation of the ER bodies at both transcriptional and post-transcriptional levels (Fig. 1). We found that *Arabidopsis* mutants

defective in either ER body biogenesis or composition are more resistant to pathogenic bacteria (Fig. 2 and S2). The main components of ER bodies are myrosinases, enzymes that modify glucosinolates to initiate the glucosinolate breakdown, which will result in different products depending on the biochemical properties of the modifier protein and the chemical nature of the glucosinolate side chain (Sugiyama and Hirai 2019; Wittstock and Burow 2010). Those products can function as defense compounds or as signaling molecules.

PYK10/BGLU23 is an atypical myrosinase similar to PENETRATION 2 (PEN2, BGLU26) that hydrolyzes indole glucosinolates (IGs) (Nakano et al. 2017; Nakazaki et al. 2019b). PEN2-mediated conversion of 4-methoxyindol-3-ylmethylglucosinolate (4MI3G) into glucosinolate-derived products plays an important role in the defense response against fungi (Bednarek et al. 2009). Interestingly, *PEN2* is required for callose deposition upon flg22 perception and for resistance against DC3000 infection in seedlings grown in liquid media (Clay et al. 2009; Johansson et al. 2014). In contrast, in adult plants grown in soil, callose deposition and DC3000 growth is not affected in the *pen2-1* mutant (Geng et al., 2012). The *pen2-1* mutant grown in soil exhibits enhanced resistance to *P. syringae* pv. *maculicola* (Stahl et al., 2016). These apparently contradictory results indicate that PEN2 activity is dependent on age and/or the metabolic state of the plant. 4MI3G overaccumulates in homogenized tissue of *bglu18/pyk10* mutants indicating that one or both of these β-glucosidases hydrolyze 4MI3G (Nakazaki et al., 2019). Our results indicate that the single *pyk10-1* mutant and the double *pyk10-1/bglu21* mutant accumulate an increased number of callose deposits in response to flg22 treatment and are more resistant to DC3000. Although both PEN2 and PYK10 seem to have the same

285 substrate (4MI3G), their respective mutants differ on phenotypes as flg22-induced callose
286 deposition and resistance to *P. syringae* DC3000 (Clay et al. 2009; Johansson et al.
287 2014). Apart from the above-mentioned effect related to growth conditions, one of the
288 reasons explaining these differences could be the different compartmentalization of both
289 PEN2 and PYK10. While PEN2 is localized in peroxisome and mitochondria (Fuchs et al.
290 2016; Lipka et al. 2005), PYK10 localizes in ER bodies (Matsushima et al. 2003).
291 Furthermore, myrosinase activity is regulated by different Myrosinase-Biding Proteins and
292 Myrosinase-Associated Proteins, as well as different specifier proteins, which lead to the
293 formation of different breakdown products (Wittstock et al. 2016). This variety of
294 compounds can have a direct or indirect effect on the plant defense response (Wittstock
295 et al. 2016).

296 In conclusion, we have demonstrated the involvement of ER body-dependent regulation
297 of immunity to bacteria and induction of ER bodies as a pathogen virulence strategy.
298 Further work will shed light on how this novel function of ER bodies influences bacterial-
299 plant interactions and pave the way for the discovery of the role of indole-glucosinolates
300 breakdown on the response against bacterial invasion in plants.

Experimental procedures

Plant material and growth conditions

A. thaliana Col-0, the transgenic line expressing GFP-HDEL (Hayashi et al., 2001) and the mutants *nai1-1* (Matsushima et al. 2003), *pyk10-1* (Nagano et al. 2008), *pyk10-1/bglu21* (Nagano et al. 2009), *bglu18-1* (Ogasawara et al. 2009) and *pbp1-1* (Nagano et al. 2005) were grown in a controlled environment chamber at 23˚C, 70% relative humidity, and a 10h/14h light/dark photoperiod with light intensity of 100µE.m^{-2}.S^{-1}. All seeds were stratified for 3-4 days at 4ºC before sowing into soil.

Bacterial strains, growth conditions and pathogen assays

Pseudomonas syringae pv. *tomato* DC3000 (Cuppels 1986) and the derivative strains Δ*hrcC* and *cor* ⁻ (cma- cfa-; (Brooks et al. 2004)) were grown at 28°C in Lysogeny Broth (LB) medium (Bertani 1951). Antibiotics were used when appropriate, at the following concentrations: Rifampicin (100 μg/ml), kanamycin (25 μg/ml) and gentamycin (10 μg/ml). The DC3000, Δ*hrcC* and *cor* ⁻ eYFP (enhanced yellow fluorescent protein) derivatives were generated using a Tn7 delivery system as previously described (Rufian et al. 2018) For pathogen assays, five-week-old *Arabidopsis* plants were inoculated with a *P. syringae* suspension of 5x10^4 CFU/mL prepared in 10 mM $MgCl_2$. Three leaves per plant were syringe infiltrated and five plants were used for each experiment. Four days after inoculation, three leaf discs of 1 cm of diameter (one per leaf were ground in 1 mL 10 mM $MgCl_2$, and serial dilutions were plated.

Transcriptomic analyses

For the analysis of NAI1 and PYK10 expression under different biotic stresses, we used transcriptomic data available in eFP Browser. Specifically, we used the dataset AtGenExpress: Response to virulent, avirulent, type III-secretion system deficient and nonhost bacteria (NASCArrays-120). 5-week-old Col-0 plants were infiltrated with the corresponding *P. syringae* strain. Samples were taken 24h after treatment and RNA was isolated and hybridized to the ATH1 GeneChip. The data were normalized by GCOS normalization, TGT 100.

flg22-related assays

For ROS burst assays, leaf discs were collected using a cork borer of 5mm diameter from three-week-old *Arabidopsis* plants and floated overnight in deionized water. The next day, the water was replaced with an assay solution containing 17 mg/ml luminol (Sigma), 10 mg/ml horse radish peroxidase (Sigma) and 100 nM flg22 (Genscript). Luminescence was measured using Tristar multimode reader (Berthold technology).

Callose deposits were quantified from four-week-old *Arabidopsis* leaves infiltrated with 10 µM flg22 solution. Eighteen hours after treatment, leaves were detached and incubated 15 minutes at 65ºC in 5 ml of alcoholic lactophenol (1 volume of phenol: glycerol: lactic acid: water (1:1:1:1) and 2 volumes of ethanol). Leaves were transferred to fresh alcoholic lactophenol and incubated overnight at room temperature. After two washes with 50% ethanol, leaves were stained with aniline blue and callose deposits were visualized under a fluorescence microscope. Quantification of callose deposits was performed using the Fiji distribution of ImageJ.

Confocal microscopy

Two-week old *Arabidopsis* GFP-HDEL plants were vacuum infiltrated with either water or 100 nM flg22. Three hours after the treatment, cotyledons were detached and observed under a Zeiss LSM710 confocal microscope equipped with a LDC-apochromat 40x/1.1W Korr M27 water-immersion objective (NA 1.1). GFP was excited at 488 nm and emission collected at 500-550 nm.

For visualization of bacterial microcolonies, five-week old *Arabidopsis* GFP-HDEL plants were syringe infiltrated with a $5x10^4$ CFU/mL suspension and leaves were visualized using the Leica SP5 II confocal microscope (Leica Microsystems GmbH, Wetzlar, Germany). Images of eYFP and GFP were sequentially obtained using the following conditions (excitation/ emission): eYFP (514 nm/ 525 to 600 nm), GFP (488/ 500 to 525 nm). Z series imaging was taken at 1 μm interval. Image processing was performed using Leica LAS AF (Leica Microsystems). ER bodies were quantified using Fiji distribution of ImageJ software.

S. exigua performance

S. exigua eggs were kindly provided by Dr. Salvador Herrero (U. Valencia). After eclosion, *S. exigua* larvae were fed with an artificial diet (Elvira et al. 2010). Three days after eclosion, five larvae of approximately same size were transferred to a four-to-five week old *Arabidopsis* plant grown in Jiffy-7 pods. Larvae were transfer to new plants every 24 hours to avoid food privation. Seven days after plant feeding, fresh weight of the larvae was measured. For each experiment, five replicates were performed (25 larvae per genotype).

ACKNOWLEDGMENTS

J.S. Rufián has been supported by a FPI fellowship associated with a grant of E.R. Bejarano (MICINN, Spain; AGL2010-22287-C02-2), funds from BIO2012-35641 (MICINN, Spain) granted to C.R. Beuzón, and Plan Propio de la Universidad de Málaga – Andalucía Tech. The work was co-funded by European Regional Development Funds (FEDER). G. Coaker is supported by grants from the National Institutes of Health (RO1GM092772, R35GM13640).

Literature Cited

Bednarek, P., Piślewska-Bednarek, M., Svatos, A., Schneider, B., Doubsky, J., Mansurova, M., Humphry, M., Consonni, C., Panstruga, R., Sanchez-Vallet, A., Molina, A., and Schulze-Lefert, P. 2009. A glucosinolate metabolism pathway in living plant cells mediates broad-spectrum antifungal defense. Pages 101-106 in: Science American Association for the Advancement of Science.

Bender, C. L., Alarcón-Chaidez, F., and Gross, D. C. 1999. Pseudomonas syringae phytotoxins: mode of action, regulation, and biosynthesis by peptide and polyketide synthetases. Microbiol Mol Biol Rev 63:266-292.

Bertani, G. 1951. Studies on lysogenesis. I. The mode of phage liberation by lysogenic Escherichia coli. Journal of bacteriology 62:293-300.

Brooks, D. M., Hernandez-Guzman, G., Kloek, A. P., Alarcon-Chaidez, F., Sreedharan, A., Rangaswamy, V., Penaloza-Vazquez, A., Bender, C. L., and Kunkel, B. N. 2004. Identification and characterization of a well-defined series of coronatine biosynthetic mutants of Pseudomonas syringae pv. tomato DC3000. Mol Plant Microbe Interact 17:162-174.

Chung, H. S., Koo, A. J. K., Gao, X., Jayanty, S., Thines, B., Jones, A. D., and Howe, G. A. 2008. Regulation and function of Arabidopsis JASMONATE ZIM-domain genes in response to wounding and herbivory. Pages 952-964 in: Plant Physiol American Society of Plant Biologists.

Cipollini, D., Enright, S., Traw, M. B., and Bergelson, J. 2004. Salicylic acid inhibits jasmonic acid-induced resistance of Arabidopsis thaliana to Spodoptera exigua. Pages 1643-1653 in: Molecular Ecology.

Clay, N. K., Adio, A. M., Denoux, C., Jander, G., and Ausubel, F. M. 2009. Glucosinolate metabolites required for an Arabidopsis innate immune response. Science 323:95-101.

Couto, D., and Zipfel, C. 2016. Regulation of pattern recognition receptor signalling in plants. Nature reviews. Immunology 16:537-552.

Cuppels, D. A. 1986. Generation and Characterization of Tn*5* Insertion Mutations in *Pseudomonas syringae* pv. *tomato*. Appl. Environ. Microbiol. 51:323-327.

Elvira, S., Gorria, N., Munoz, D., Williams, T., and Caballero, P. 2010. A simplified low-cost diet for rearing Spodoptera exigua (Lepidoptera: Noctuidae) and its effect on S. exigua nucleopolyhedrovirus production. J Econ Entomol 103:17-24.

Fuchs, R., Kopischke, M., Klapprodt, C., Hause, G., Meyer, A. J., Schwarzländer, M., Fricker, M. D., and Lipka, V. 2016. Immobilized Subpopulations of Leaf Epidermal Mitochondria Mediate PENETRATION2-Dependent Pathogen Entry Control in Arabidopsis. Pages 130-145 in: The Plant Cell … American Society of Plant Biologists.

Geng, X., Cheng, J., Gangadharan, A., and Mackey, D. 2012. The coronatine toxin of Pseudomonas syringae is a multifunctional suppressor of Arabidopsis defense. Pages 4763-4774 in: The Plant Cell ….

Gimenez-Ibanez, S., Boter, M., Ortigosa, A., García-Casado, G., Chini, A., Lewsey, M. G., Ecker, J. R., Ntoukakis, V., and Solano, R. 2017. JAZ2 controls stomata dynamics during bacterial invasion. Pages 1378-1392 in: New Phytol.

Gómez-Gómez, L., and Boller, T. 2000. FLS2: an LRR receptor-like kinase involved in the perception of the bacterial elicitor flagellin in Arabidopsis. Mol Cell 5:1003-1011.

Henry, E., Yadeta, K. A., and Coaker, G. 2013. Recognition of bacterial plant pathogens: local, systemic and transgenerational immunity. New Phytol 199:908-915.

Johansson, O. N., Fantozzi, E., Fahlberg, P., Nilsson, A. K., Buhot, N., Tör, M., and Andersson, M. X. 2014. Role of the penetration-resistance genes PEN1, PEN2and PEN3in the hypersensitive response and race-specific resistance in Arabidopsis thaliana. Pages 466-476 in: Plant J.

Lahrmann, U., Strehmel, N., Langen, G., Frerigmann, H., Leson, L., Ding, Y., Scheel, D., Herklotz, S., Hilbert, M., and Zuccaro, A. 2015. Mutualistic root endophytism is not associated with the reduction of saprotrophic traits and requires a noncompromised plant innate immunity. New Phytol 207:841-857.

Lipka, V., Dittgen, J., Bednarek, P., Bhat, R., Wiermer, M., Stein, M., Landtag, J., Brandt, W., Rosahl, S., Scheel, D., Llorente, F., Molina, A., Parker, J., Somerville, S., and Schulze-Lefert, P. 2005. Pre- and postinvasion defenses both contribute to nonhost resistance in Arabidopsis. Pages 1180-1183 in: Science American Association for the Advancement of Science.

Macho, A. P. 2015. Subversion of plant cellular functions by bacterial type-III effectors: beyond suppression of immunity. New Phytol.

Matsushima, R., Fukao, Y., Nishimura, M., and Hara-Nishimura, I. 2004. NAI1 gene encodes a basic-helix-loop-helix-type putative transcription factor that regulates the formation of an endoplasmic reticulum-derived structure, the ER body. Pages 1536-1549 in: THE PLANT CELL ONLINE American Society of Plant Biologists.

Matsushima, R., Hayashi, Y., Kondo, M., Shimada, T., Nishimura, M., and Hara-Nishimura, I. 2002. An endoplasmic reticulum-derived structure that is induced under stress conditions in Arabidopsis. Pages 1807-1814 in: Plant Physiol American Society of Plant Biologists.

Matsushima, R., Hayashi, Y., Yamada, K., Shimada, T., Nishimura, M., and Hara-Nishimura, I. 2003. The ER body, a novel endoplasmic reticulum-derived structure in Arabidopsis. Pages 661-666 in: Plant Cell Physiol.

Melotto, M., Underwood, W., and He, S. Y. 2008. Role of stomata in plant innate immunity and foliar bacterial diseases. Annu Rev Phytopathol 46:101-122.

Melotto, M., Underwood, W., Koczan, J., Nomura, K., and He, S. Y. 2006. Plant stomata function in innate immunity against bacterial invasion. Cell 126:969-980.

Millet, Y. A., Danna, C. H., Clay, N. K., and Songnuan, W. 2010. Innate immune responses activated in Arabidopsis roots by microbe-associated molecular patterns. in: The Plant Cell ….

Mitsuhashi, N., Shimada, T., Mano, S., Nishimura, M., and Hara-Nishimura, I. 2000. Characterization of organelles in the vacuolar-sorting pathway by visualization with GFP in tobacco BY-2 cells. Plant Cell Physiol 41:993-1001.

Müller, R., de Vos, M., Sun, J. Y., Sønderby, I. E., Halkier, B. A., Wittstock, U., and Jander, G. 2010. Differential Effects of Indole and Aliphatic Glucosinolates on Lepidopteran Herbivores. Pages 905-913 in: J Chem Ecol.

Nagano, A. J., Matsushima, R., and Hara-Nishimura, I. 2005. Activation of an ER-body-localized beta-glucosidase via a cytosolic binding partner in damaged tissues of Arabidopsis thaliana. Pages 1140-1148 in: Plant Cell Physiol.

Nagano, A. J., Fukao, Y., Fujiwara, M., Nishimura, M., and Hara-Nishimura, I. 2008. Antagonistic jacalin-related lectins regulate the size of ER body-type beta-glucosidase complexes in Arabidopsis thaliana. Pages 969-980 in: Plant Cell Physiol.

Nagano, A. J., Maekawa, A., Nakano, R. T., Miyahara, M., Higaki, T., Kutsuna, N., Hasezawa, S., and Hara-Nishimura, I. 2009. Quantitative analysis of ER body morphology in an Arabidopsis mutant. Pages 2015-2022 in: Plant Cell Physiol.

Nakano, R. T., Yamada, K., Bednarek, P., Nishimura, M., and Hara-Nishimura, I. 2014a. ER bodies in plants of the Brassicales order: biogenesis and association with innate immunity. Front Plant Sci 5:73.

Nakano, R. T., Yamada, K., Bednarek, P., Nishimura, M., and Hara-Nishimura, I. 2014b. ER bodies in plants of the Brassicales order: biogenesis and association with innate immunity. Page 73 in: Front. Plant Sci. Frontiers.

Nakano, R. T., Piślewska-Bednarek, M., Yamada, K., Edger, P. P., Miyahara, M., Kondo, M., Böttcher, C., Mori, M., Nishimura, M., Schulze-Lefert, P., Hara-Nishimura, I., and Bednarek, P. 2017. PYK10 myrosinase reveals a functional coordination between endoplasmic reticulum bodies and glucosinolates in Arabidopsis thaliana. Pages 204-220 in: Plant J.

Nakazaki, A., Yamada, K., Kunieda, T., Tamura, K., Hara-Nishimura, I., and Shimada, T. 2019a. Biogenesis of leaf endoplasmic reticulum body is regulated by both jasmonate-dependent and independent pathways. Pages 1-3 in: Plant Signaling & Behavior Taylor & Francis.

Nakazaki, A., Yamada, K., Kunieda, T., Sugiyama, R., Hirai, M. Y., Tamura, K., Hara-Nishimura, I., and Shimada, T. 2019b. Leaf Endoplasmic Reticulum Bodies Identified in Arabidopsis Rosette Leaves Are Involved in Defense against Herbivory. Pages 1515-1524 in: Plant Physiol.

Ogasawara, K., Yamada, K., Christeller, J. T., Kondo, M., Hatsugai, N., Hara-Nishimura, I., and Nishimura, M. 2009. Constitutive and inducible ER bodies of Arabidopsis thaliana accumulate distinct beta-glucosidases. Pages 480-488 in: Plant Cell Physiol.

Rehrig, E. M., Appel, H. M., Jones, A. D., and Schultz, J. C. 2014. Roles for jasmonate- and ethylene-induced transcription factors in the ability of Arabidopsis to respond differentially to damage caused by two insect herbivores. Page 407 in: Front. Plant Sci. Frontiers.

Rufian, J. S., Macho, A. P., Corry, D. S., Mansfield, J. W., Ruiz-Albert, J., Arnold, D. L., and Beuzon, C. R. 2018. Confocal microscopy reveals in planta dynamic interactions between pathogenic, avirulent and non-pathogenic Pseudomonas syringae strains. Molecular plant pathology 19:537-551.

Santamaría, M. E., Martinez, M., Arnaiz, A., Ortego, F., Grbic, V., and Diaz, I. 2017. MATI, a Novel Protein Involved in the Regulation of Herbivore-Associated Signaling Pathways. Pages 80-18 in: Front. Plant Sci.

Sherameti, I., Venus, Y., Drzewiecki, C., Tripathi, S., Dan, V. M., Nitz, I., Varma, A., Grundler, F. M., and Oelmüller, R. 2008. PYK10, a beta-glucosidase located in the

endoplasmatic reticulum, is crucial for the beneficial interaction between Arabidopsis thaliana and the endophytic fungus Piriformospora indica. Pages 428-439 in: Plant J. Blackwell Publishing Ltd.

Sugiyama, R., and Hirai, M. Y. 2019. Atypical Myrosinase as a Mediator of Glucosinolate Functions in Plants. Page 1008 in: Front. Plant Sci. Frontiers.

Thilmony, R., Underwood, W., and He, S. Y. 2006. Genome-wide transcriptional analysis of the Arabidopsis thaliana interaction with the plant pathogen Pseudomonas syringae pv. tomato DC3000 and the human pathogen Escherichia coli O157:H7. Plant J 46:34-53.

Van Oosten, V. R., Bodenhausen, N., Reymond, P., Van Pelt, J. A., Van Loon, L. C., Dicke, M., and Pieterse, C. M. J. 2008. Differential effectiveness of microbially induced resistance against herbivorous insects in Arabidopsis. Pages 919-930 in: Mol. Plant Microbe Interact. The American Phytopathological Society.

Weiler, E. W., Kutchan, T. M., Gorba, T., Brodschelm, W., Niesel, U., and Bublitz, F. 1994. The Pseudomonas phytotoxin coronatine mimics octadecanoid signalling molecules of higher plants. FEBS letters 345:9-13.

Wittstock, U., and Burow, M. 2010. Glucosinolate Breakdown in Arabidopsis: Mechanism, Regulation and Biological Significance. Pages e0134-0114 in: The Arabidopsis Book.

Wittstock, U., Kurzbach, E., Herfurth, A. M., and Stauber, E. J. 2016. Glucosinolate Breakdown. Pages 125-169 in: Advances in Botanical Research Elsevier Ltd.

Xu, Z., Escamilla-Trevino, L., Zeng, L., Lalgondar, M., Bevan, D., Winkel, B., Mohamed, A., Cheng, C. L., Shih, M. C., Poulton, J., and Esen, A. 2004. Functional genomic analysis of Arabidopsis thaliana glycoside hydrolase family 1. Plant Mol Biol 55:343-367.

Yamada, K., Hara-Nishimura, I., and Nishimura, M. 2011. Unique defense strategy by the endoplasmic reticulum body in plants. Pages 2039-2049 in: Plant Cell Physiol.

Yamada, K., Nagano, A. J., Nishina, M., Hara-Nishimura, I., and Nishimura, M. 2008. NAI2 is an endoplasmic reticulum body component that enables ER body formation in Arabidopsis thaliana. Pages 2529-2540 in: THE PLANT CELL ONLINE American Society of Plant Biologists.

Figures and Fig Legends

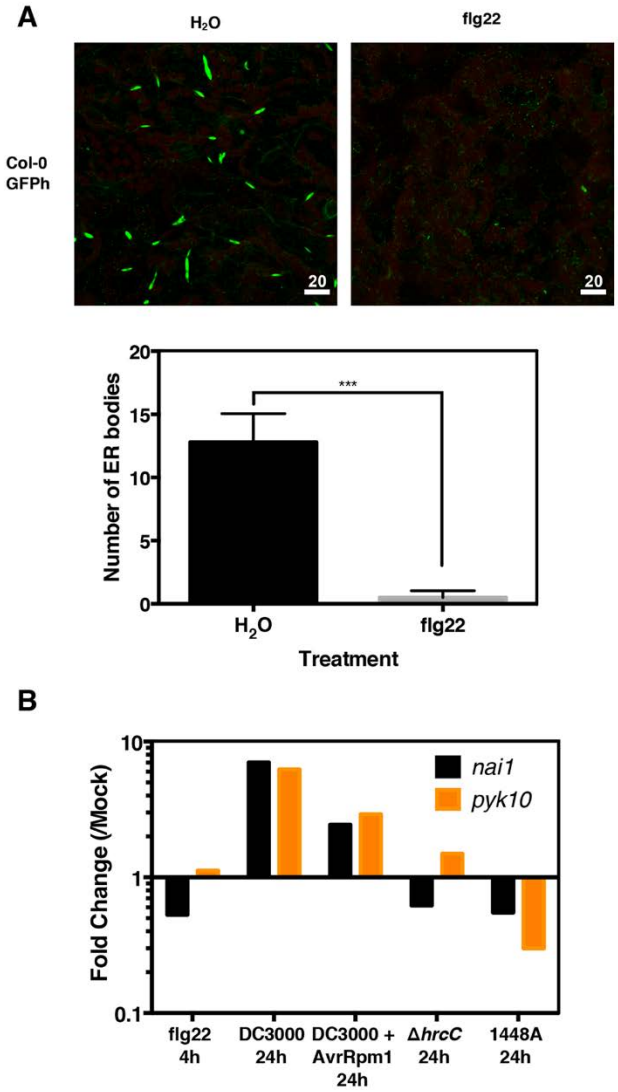

Figure 1. ER bodies are downregulated after activation of PTI.
(**A**) Constitutive ER bodies disappear after flg22 treatment. Two-week-old *Arabidopsis* GFP-HDEL plants were vacuum infiltrated with water or 100 nM flg22. Cotyledons were observed in a confocal microscope three hours after treatment. For ER body quantification, three fields from three independent cotyledons were used. ER bodies were quantified using Fiji. The experiment was repeated four times with similar results and a mean value ± SE of all quantifications is shown. Statistical differences were determined with a two-tailed t-test comparing water treatment with flg22. Three asterisks indicate $p<0.001$. Scale bar: 20 µm. (**B**) Expression patterns of *nai1* and *pyk10* genes under different biotic stress. Data was obtained from available microarray in eFP Browser. Five week-old Col-0 plant leaves were syringe-infiltrated with either a 1 µM flg22 solution (using water as mock treatment) or the indicated bacterial strain at 10^8 cfu/ml (using 10 mM $MgCl_2$ as mock treatment). Samples were taken 24 hours after treatment. Fold change relative to mock treatment is shown.

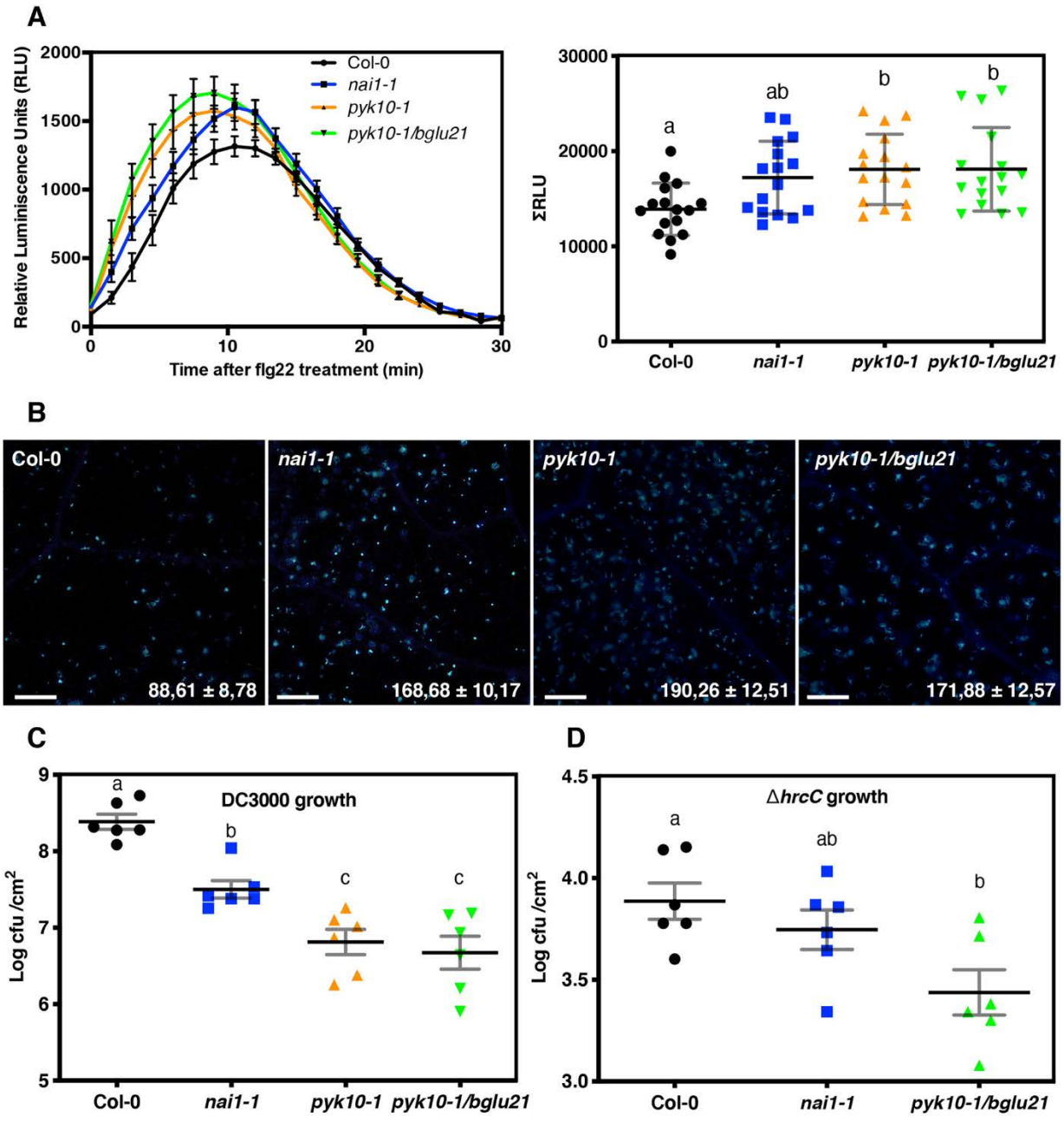

Figure 2. ER body mutants exhibit enhanced resistance against *P. syringae*. (A) flg22-induced ROS burst in Col-0, *nai1-1*, *pyk10-1* and *pyk10-1/bglu21*. Three-week-old *Arabidopsis* leaf discs were treated with 100 nM flg22 and ROS was quantified using a luminescence based assay. The left graph represent the dynamics of the ROS produced in the different genotypes and the right graph represent the total relative lights units (RLU) detected over a 30 minutes period. Error bars indicate SD, $n = 16$. Statistically differences were determined with one-way ANOVA ($\alpha = 0.05$) with Tukey's multiple comparisons test and different letters indicate statistical significance. The experiment was repeated four times with similar results and a representative experiment is shown. (**B**) Quantification of flg22-induced callose deposition in Col-0, *nai1-1*, *pyk10-1* and *pyk10-1/bglu21.* Four-week-old plants were infiltrated with 10 µM flg22 and callose deposits were visualized

under an epifluorescence microscope eighteen hours after treatment. Four images were taken per leaf and nine leaves were used per experiment. The mean number of deposits was quantified and is included ± SE in the bottom-right corner of each representative image. The experiment was repeated three times with similar results, and a representative experiment is shown. White bar: 100 µm. (**C**) Growth of *P. syringae* pv. *tomato* DC3000 in Col-0, *nai1-1*, *pyk10-1* and *pyk10-1/bglu21.* Five-week-old plant leaves were syringe inoculated with a suspension of $5x10^4$ CFU/mL. Four days after inoculation, bacteria were recovered and quantified. Values for each individual plant are shown (*n*=6). Bars represent the mean value ± SE. Statistically differences were determined with one-way ANOVA (α = 0.05) with Tukey's multiple comparisons test and different letters indicate statistical significance. The experiment was repeated four times with similar results, and a representative experiment is shown. (**D**) Growth of the *P. syringae* pv. *tomato* Δ*hrcC* derivative in Col-0, *nai1-1*, and *pyk10-1/bglu21.* Five-week-old plant leaves were syringe inoculated with a suspension of $5x10^4$ CFU/mL. Four days after inoculation, bacteria were recovered and quantified. Values for each individual plant are shown (*n*=6). Bars represent the mean value ± SE. Statistically differences were determined with one-way ANOVA (α= 0.05) with Tukey's multiple comparisons test and different letters indicate statistical significance. The experiment was repeated two times with similar results, and a representative replicate is shown.

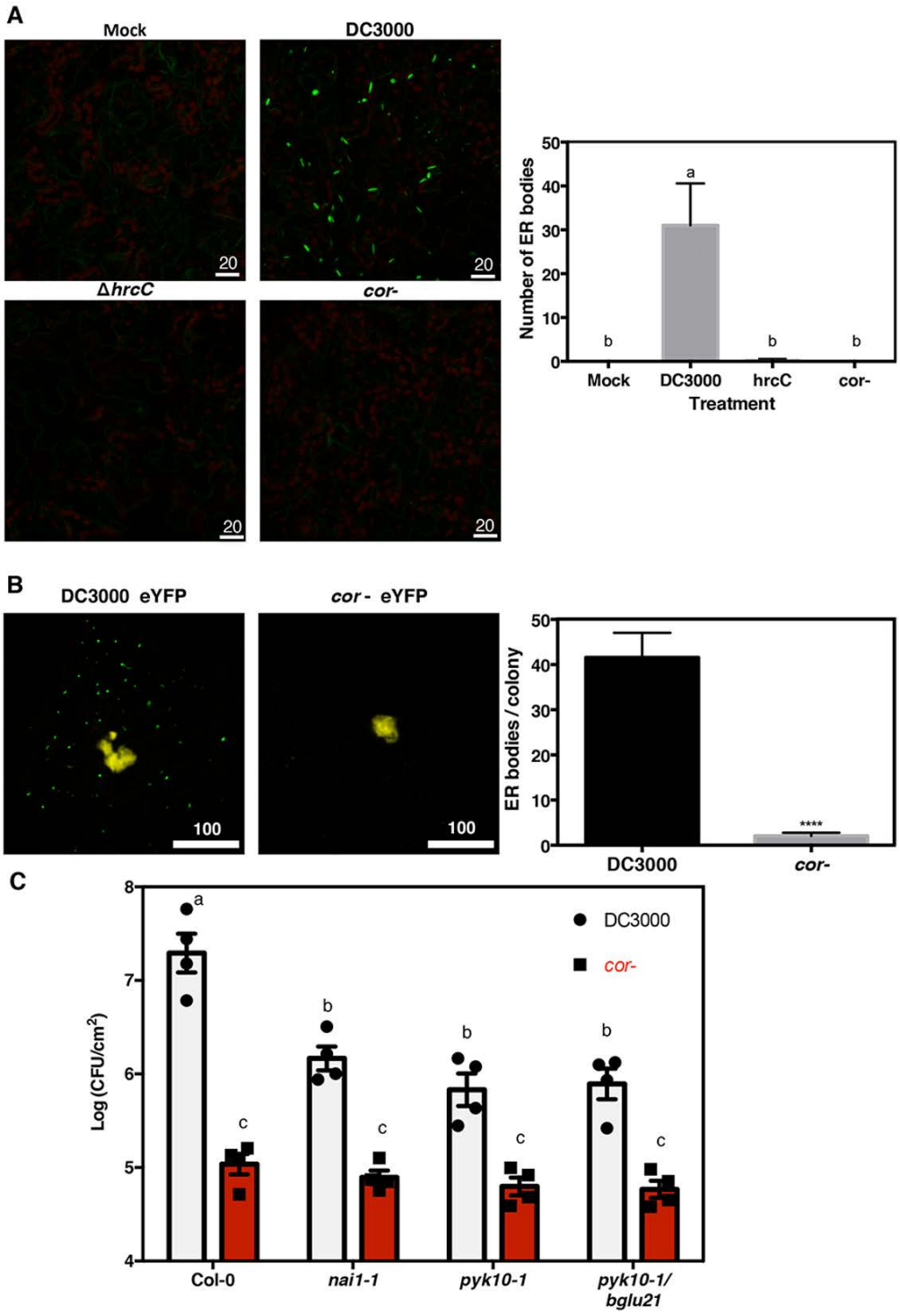

Figure 3. Coronatine induces formation of ER bodies in leaves and its virulence function is compromised in mutants impaired in ER body formation.

(**A-B**) Confocal microscope images of bacterial micro-colonies (yellow) and ER bodies (green). Five-week-old *Arabidopsis* GFP-HDEL plants were syringe inoculated with a bacterial suspension containing 5x10^4 CFU/mL. Three days after inoculation, leaf sections were visualized under the confocal microscope. A representative z-stack projection image is shown. ER bodies were quantified from the green channel using Fiji.

603 Bars represent the mean number of ER bodies in (A) or the number of ER bodies
604 surrounding a single bacterial micro colony in (B) ± SE. The experiments were repeated
605 three times with similar results, and the mean of all experiments is shown. ER bodies
606 were quantified using Fiji and statistically differences were determined with one-way
607 ANOVA (α= 0.05) with Tukey's multiple comparison test in (A) and different letters indicate
608 statistical significance. In (B) data were analyzed by a t-test (α= 0.001). White bar: 20 µm.
609 (**C**) Growth of *P. syringae* pv. *tomato* DC3000 and its derivative coronatine mutant (*cor* -
610) in Col-0, *nai1-1*, *pyk10-1* and *pyk10-1/bglu21.* Five-week-old plant leaves were syringe
611 inoculated with a bacterial suspension of $5x10^4$ CFU/mL. Four days after inoculation,
612 bacteria were recovered and quantified. Values for each individual plant are shown (*n*=6).
613 Bars represent the mean value ± SE. Statistically differences were determined with one-
614 way ANOVA (α= 0.05) with Tukey's multiple comparisons test and different letters indicate
615 statistical significance. The experiment was repeated three times with similar results, and
616 a representative experiment is shown.

617

618

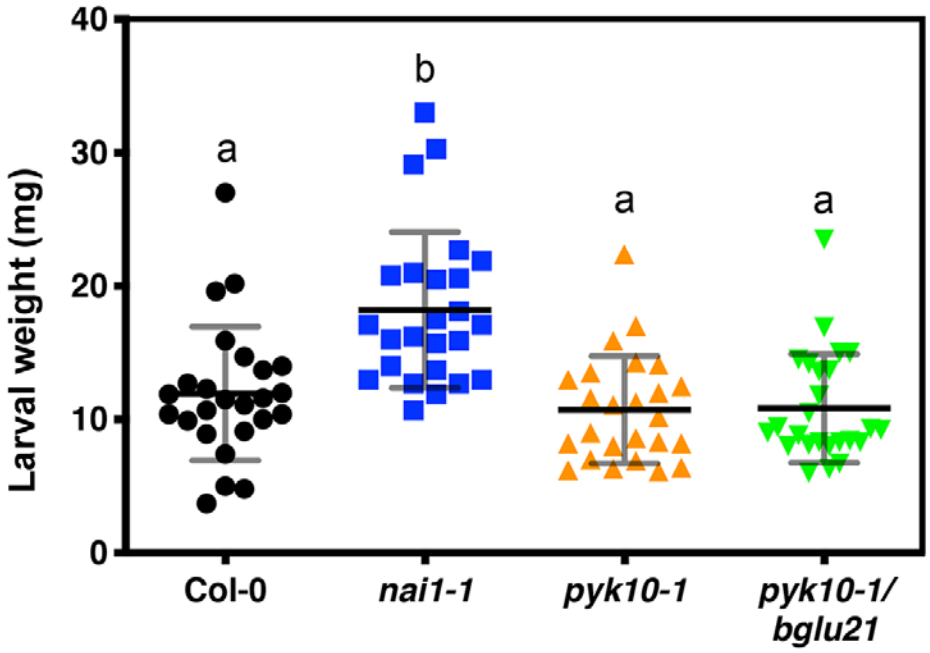

Figure 4. *Spodoptera exigua* performance is improved in the *nai1-1* mutant. Three-week-old *Arabidopsis* Col-0, *nai1-1*, *pyk10-1* and *pyk10-1/bglu21* plants were challenged with three-days-old *S. exigua* larvae. Seven days after feeding, fresh weight of each larva was measured. Bars represent the mean weight ± SE (*n*=20). Statistically differences were determined with one-way ANOVA (α= 0.05) with Tukey's multiple comparisons test and different letters indicate statistical significance. The experiment was repeated three times with similar results, and a representative experiment is shown.

Supplemental Figure Legends

Figure S1. No ER bodies are present in *nai1-1* cotyledons.

Two-week-old *Arabidopsis nai1-1* GFP-HDEL plants were vacuum infiltrated with water or 100 nM flg22. Cotyledons were observed in a confocal microscope three hours after treatment. White bar: 20 µm.

Figure S2. *bglu18-1* and *pbp1-1* show enhanced resistance to *P. syringae*

(**A**) Flg22-induced ROS burst in Col-0, *bglu18-1*, and *pbp1-1*. Three-week-old *Arabidopsis* leaf discs were treated with 100 nM flg22 and ROS was quantified using a luminescence based assay. Error bars indicate ±SE, *n* = 16. The experiment was repeated twice with similar results and a representative experiment is shown. (**B**) Growth of *P. syringae* pv. *tomato* DC3000 in Col-0, *bglu18-1*, and *pbp1-1.* Five-week-old plant leaves were syringe inoculated with a suspension of $5x10^4$ CFU/mL. Four days after inoculation, bacteria were recovered and quantified. Values for each individual plant are shown (*n*=6). Bars represent the mean value ± SE. Statistically differences were determined with one-way ANOVA (α= 0.05) with Tukey's multiple comparisons test and different letters indicate statistical significance. The experiment was repeated twice with similar results and a representative experiment is shown.

Figure S3. Coronatine induce the expression of ER body and indole glucosinolate related genes.

(A) Transcriptomic analysis of several genes related with ER bodies formation or indole-glucosinolate metabolism. Bars show Log_2 signal values from microarrays datasets. Data was obtained from the study by Thilmony et al. (2006), available in Genevestigator. *Arabidopsis* Col-5 leaves were inoculated with water (Mock), or a 10^6 cfu/ml suspension of DC3000 or DC3118 (cor^-). Samples were taken 24 hours after inoculation. (B) Coexpression analyses of PYK10 (At3G09260). Analyses were performed using ATTED-II software.